2024 European Control Conference (ECC)
June 25-28, 2024. Stockholm, Sweden

Logarithmic Feedback Control of Passive Interference

Torbjörn Wigren

Abstract— **Passive intermodulation interference in wireless systems is caused by downlink radio transmissions that are nonlinearly mixed and frequency shifted in close conductive objects. This interference may jam uplink receivers. The paper proposes mitigation by logarithmic feedback control using downlink transmission power actuation. The nonlinear single downlink feedback loop is proved to be globally stable provided that a loop-gain-loop-delay stability condition holds. The multi downlink problem is then addressed by derivation of a degree greedy multiple-input-single-output controller that is proved to be optimal in a static sense. Simulations using measured data traffic illustrate the performance of the control systems.**

I. Introduction

The paper proposes new, globally stable feedback regulation of passive intermodulation (PIM) disturbances in wireless systems. The regulation is achieved by carrier transmit power actuation in the downlink (DL), to mitigate the PIM disturbances in an uplink (UL) receiver at a site. PIM may be created in the radio itself, as well as in close conductive and magnetic objects like loose connectors or rusty metal objects littering the site close to the transmit antennas. Currents induced by *multiple* radio transmissions may mix nonlinearly in such PIM sources, thereby creating frequency shifted PIM radio signals. In case the frequency shifted PIM signals are within the frequency band of a receiver, the UL may be interfered [3], [6], [8], [12].

In case the receiver antenna has more than one element a receiver null can be formed against a point-wise PIM source using interference rejection combining (IRC), [4], [13]. In addition, large antenna arrays can be used to avoid DL transmission in the direction of a PIM source with null forming, [11]. The disadvantages are that suppression of other UL interference competes with the need to reduce PIM, and that the coverage and user throughput in the direction of the PIM source are compromised. Another well known mitigation technique is denoted PIM cancellation. For example, a truncated Volterra series model of the PIM signal can be obtained by techniques described in [9]. Estimation of the Volterra channel, followed by subtraction of the predicted PIM signal from the measured uplink signal can then reduce the effect of the PIM disturbance. However, PIM cancellation is demanding, computationally and from an interface perspective. The reasons are the many super-linear terms, that also lead to high bandwidth signalling of over-sampled signals between carriers.

Torbjörn Wigren is with the BNEW TS ST, Ericsson AB, SE-16480 Stockholm, Sweden. He is also with the Department of Information Technology, Uppsala University, Box 337, SE-75105 Uppsala, SWEDEN `torbjorn.wigren @ { ericsson.com, it.uu.se }`.

When the above techniques are unavailable, the DL transmit powers need to be reduced at the expense of a reduced DL throughput. Such techniques are known as PIM avoidance (PIM-A). The paper first contributes to PIM-A with feedback control of the UL PIM power by actuation (muting) of the momentary DL transmission bandwidth of a single carrier. By a transformation to the logarithmic power domain, the PIM channel is removed from the loop gain. Application of integrating feedback control then avoids computationally intense PIM channel estimation. The second contribution uses the circle criterion [18] to derive a global loop-gain-loop-delay stability condition that is only a function of the degree of the regulated carrier in the PIM product, the controller parameters and the loop delay. The paper then extends the single-input-single-output (SISO) feedback controller to a solution of the multi-input-single-output (MISO) feedback control problem, guided by a solution of an optimization problem. The resulting degree greedy algorithm distributes the muting between the DL carriers and forms the third contribution of the paper. Finally, the performance of the SISO and MISO feedback controllers are evaluated and compared using simulated and measured data. Alternative PIM-A solutions include the use of model predictive control [5], or to apply reinforcement learning [17]. However, the guaranteed global stability would then be lost. This serves to motivate the proposed integrating feedback loop, since stability is an absolute requirement in a widely deployed commercial control system.

Variables with an overhead bar denote signals in the linear domain, while the lack of an overhead bar denote signals in the logarithmic domain. Time is denoted t, while s is the Laplace transform variable. The paper begins with a brief review of PIM in Section II, followed by the derivation of the logarithmic SISO feedback controller in Section III. Global stability is proved in Section IV, and the degree greedy algorithm is derived in Section V. A performance evaluation is reported in Section VI. Conclusions close the paper in Section VII.

II. Passive intermodulation model

To develop a model of the PIM radio signal power, a combination of stochastic differential equations [10] that describe signals and channels, and a static nonlinear function describing the PIM source may be used. When the static nonlinear function is expanded according to the Stone-Weierstrass theorem [15], [16], a truncated Volterra series model results [9]. This model decomposes the PIM signal into multiple terms each indexed by a selection of the K-tuple $n_1, ..., n_K$, where each n_k is the exponent of radio

carrier k, cf. (1). The PIM degree n is the maximum value of $\sum_{k=1}^{K} n_k$, evaluated over all terms in the PIM model. A PIM signal of degree n thus consists of a sum of channel weighted products of carrier signals raised to a certain exponent, where each product is such that the sum of all exponents does not exceed n. This means that the generated PIM power of a particular term in the sum can be expressed as

$$\bar{P}_p(t) = \left|\bar{h}_p\right|^2(t) \prod_{k=1}^{K} \left(\bar{P}_k(t)\right)^{n_k}, \ \sum_{k=1}^{K} n_k \leq n. \quad (1)$$

where $\left|\bar{h}_p\right|^2(t)$ is the PIM channel power and $\bar{P}_k(t)$ is the transmit power of carrier k. The subscript $_p$ refers to the PIM generation.

III. Single radio carrier

A. Fundamental PIM assumptions

The approach of the paper is based on the assumption that

A1) There is a dominating PIM power term.

Since A1 is an approximation building on (1), there will be modeling errors as formalized by

A2) $\tilde{\bar{P}}_p(t)$ is a multiplicative model error acting on the dominating PIM power term.

The model A2 is selected to obtain an additive error in the logarithmic domain. There stable integrating control will be applied to attenuate $\tilde{P}_p(t)$.

B. PIM model and Logarithmic Feedback Control

The PIM model for *single DL carrier* regulation defined by A1, A2 and (1) can be represented as

$$\bar{P}_p(t) = \left|\bar{h}_p\right|^2(t) \times \left(\bar{q}_{k_p}(t)\bar{P}_{k_p,max}\right)^{n_{k_p}} \left(\prod_{k_p \neq k=1}^{K} \left(\bar{P}_k(t)\right)^{n_k}\right) \tilde{\bar{P}}_p(t). \quad (2)$$

Here the muting factor $\bar{q}_{k_p}(t) \in [\bar{q}_{k_p,min}, 1]$ is introduced since the actuator mechanism defined below is selected to limit the transit power with respect to the maximum DL carrier power, by means of a scheduling actuating threshold on the scheduled DL data bandwidth.

The PIM channel gain is computationally intense to estimate, and the model error is unknown by definition. It is therefore undesirable to have these quantities as factors of a loop gain that determines stability. This observation together with A2 suggests the first main contribution of the paper which is to perform feedback control in the logarithmic domain. It follows from (2) that

$$P_p(t) = 10\log_{10}(\bar{P}_p(t)) = n_{k_p} q_{k_p}(t) + |h_p|^2(t) + n_{k_p} P_{k_p,max} + \sum_{k_p \neq k=1}^{K} n_k P_k(t) + \tilde{P}_p(t). \quad (3)$$

Note that all quantities of (3) are in decibels (dBs), thereby avoiding multiple factors of 10. As can be seen the only remaining term of (3) in the feedback loop of Fig. 1 that is related to PIM regulation is $n_{k_p} q_{k_p}(t)$. All other signals related to PIM generation are additive and do no longer affect the loop gain, and thereby the stability. The integrating controller used below will attempt to regulate away all these additive disturbances.

The handling of other interference $I(t)$ from neighbor cell UEs (mobiles) plus thermal noise $N(t)$ needs the assumption

A3) The effect of $\bar{I}(t)$ and $\bar{N}(t)$ can be approximated with addition in the logarithmic domain.

This is admittedly a modeling approximation, needed for further control system design and stability analysis. It is believed to be reasonable in the normal case when the reference value ΔP_p^{ref} of the control loop is set to give a remaining PIM power a few dBs *above* the other interference, and since it is this PIM power excess that is the measured feedback signal. This means that when the feedback loop operates as intended the following motivation for A3 holds

$$\begin{aligned} &10\log_{10}\left(\bar{P}_p(t) + \bar{I}(t) + \bar{N}(t)\right) \\ &\approx 10\log_{10}\left(10^{\frac{\Delta P_p^{ref}}{10}}\left(\bar{I}(t) + \bar{N}(t)\right) + \bar{I}(t) + \bar{N}(t\right) \\ &= 10log_{10}\left(10^{\frac{\Delta P_p^{ref}}{10}} + 1\right) + \left(I(t) + N(t)\right). \end{aligned} \quad (4)$$

Here $I(t) + N(t)$ needs to be treated as one signal.

C. Control Objective

The UL is always subject to other interference given by $I(t) + N(t)$. This limits the capacity according to Shannons theorem [4]. When PIM is present and adds to the denominator of the signal to noise ratio, this leads to the conclusion that the control objective should be to control the PIM power to be of the same size as $I(t) + N(t)$. If the passive disturbance power would be much higher, the UL throughput and capacity would be negatively affected, and in case the passive disturbance power would be controlled to be much below $I(t)+N(t)$ the DL throughput and capacity would be unnecessarily reduced. This is handled by the configurable reference value $\Delta P_p^{ref}(t)$ that appears in Fig. 1.

D. Feedback Measurement and Delays

To meet the control objective, it is necessary to measure the PIM power level *with respect to* $(I(t) + N(t))$ in the UL. Such a measurement can be constructed using the standard UL interference measurements, by the introduction of occasional and infrequent complete muting (blanking) of the DL, zeroing one factor of (1) thereby creating an UL signal free of PIM. The *PIM power excess* is then

$$\begin{aligned} \Delta P_p(t) &= P_p(t) + I(t) + N(t) - \left(I(t_{blank}) + N(t_{blank})\right) \\ &= P_p(t) + I(t) + N(t) - \Delta P_{blank}(t). \end{aligned} \quad (5)$$

Here $\Delta P_{blank}(t)$ denotes the total interference at the last blanking occasion t_{blank}.

There is a scheduling delay, $c_{k_p} T_s$, before DL control and blanking commands take effect on the UL, where T_S is the sampling period. There is also a feedback signalling delay $f_{k_p} T_s$. Here c_{k_p} and f_{k_p} are fractional numbers.

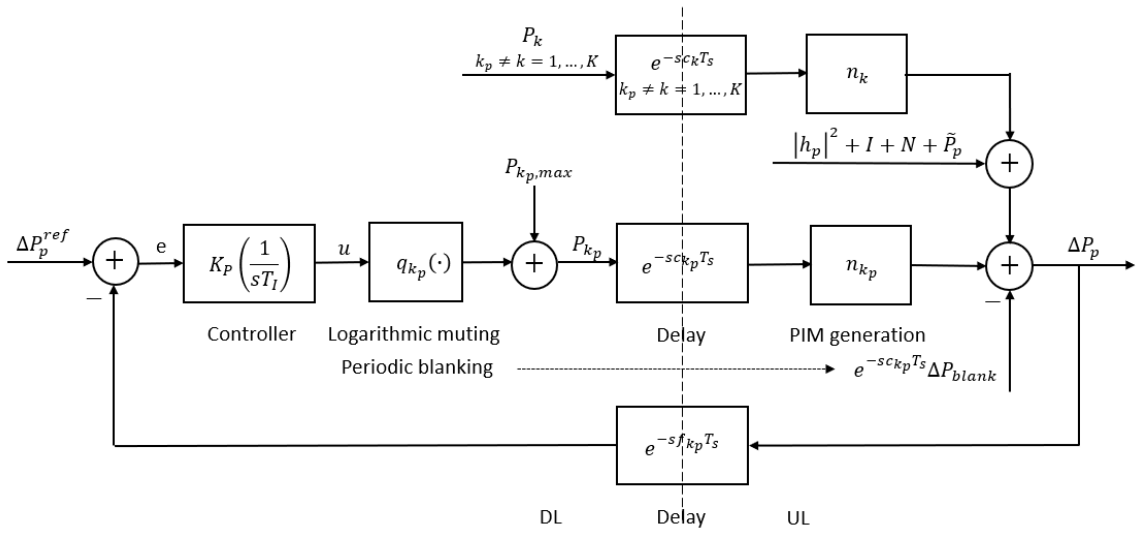

Fig. 1. Block diagram of the single carrier PIM power feedback control system, operating in the logarithmic domain.

E. Actuator Mechanism

In 4G and 5G systems the transmission is defined on a time-frequency grid, where the duration of a transmission time interval (TTI) is further divided into symbols [1]. The frequency band is divided into sub-carriers frequencies. Each time frequency point in the grid represents a complex data symbol. For each TTI, the resources are combined into physical resource blocks (PRBs) that cover a certain part of the frequency bandwidth. The PRBs are further grouped into resource block groups (RBGs) that form the smallest DL data item. There is therefore quantization effects on the DL PIM power actuation quantity $q_{k_p}(\cdot)$. The DL carrier power is typically directly proportional to the number of scheduled RBGs. Together with the transformation to the logarithmic domain, this means that $q_{k_p}(\cdot)$ will be a logarithmic quantizer of the control signal $u(t)$, where the control signal is defined to be the negative number of scheduled PRBs. The reason for this definition is the need to obtain a sector condition in line with the circle criterion applied in Section IV. Despite the fact that $u(t)$ is not a logarithmic quantity, a notation without an overhead bar is used below. The above discussion gives

$$q_{k_p}(u(t)) = \begin{cases} 0.0, & u(t) \geq u_{k_p,max} \\ q_{k_p,u}(u(t)), & u_{k_p,min} \leq u(t) < u_{k_p,max} \\ q_{k_p,min} & u(t) < u_{k_p,min}, \end{cases} \tag{6}$$

$$u_{k_p,min} = \left(m_{k_p,min} - m_{k_p,max}\right) Q_{k_p,PRB} \tag{7}$$

$$u_{k_p,max} = -Q_{k_p,PRB} \tag{8}$$

$$q_{k_p,min} = 10\log_{10}\left|\frac{m_{k_p,min}+1}{m_{k_p,max}}\right| \tag{9}$$

$$q_{k_p,u}(u(t)) = 10\log_{10}\left|\frac{\lfloor (u(t) + (m_{k_p,max}+1)Q_{k_p,PRB})/Q_{k_p,PRB}\rfloor}{m_{k_p,max}}\right|. \tag{10}$$

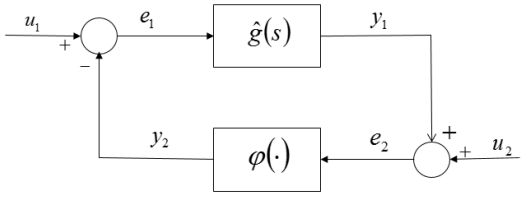

Fig. 2. The block diagram for which the circle criterion holds.

Here $Q_{k_p,PRB}$, $m_{k_p,min}$ and $m_{k_p,max}$ denote the number of PRBs per RBG, as well as the minimum and maximum number of RBGs allowed to be muted for PIM-A, respectively.

F. Integrating Controller

To regulate away biased disturbances, modeling errors and noise, the following integrating controller is applied [2]

$$C(s) = \frac{K_P}{T_I}\frac{1}{s}, \tag{11}$$

The parametrization with both a proportional gain $K_P > 0$ and an integration time $T_I > 0$ enables a very intuitive tuning of the loop gain based on the stability analysis of the next section.

IV. Global $\mathcal{L}_2$ Stability

A. The circle criterion

Since Fig. 1 contains delay and a static nonlinearity, the input-output version of the circle criterion can be applied for stability analysis [18]. The circle criterion holds for the system of Fig. 2 under the standard definitions of input-output stability theory, see [18] for all details. In Fig. 2, $\hat{g}(s)$ is the loop gain, $\varphi(\cdot)$ the static nonlinearity, u_1 and u_2 the inputs, e_1 and e_2 the error signals, while y_1 and y_2 are the outputs. The circle criterion is given by:

Lemma 1 (Circle Criterion, zero lower sector limit, [18] Theorem 6.7.8): Consider the system of Fig. 2, where

$$\hat{g}(s) = \hat{g}_a(s) + \sum_{i=0}^{\infty} g_i e^{-isT} + \frac{\hat{n}(s)}{\hat{d}(s)},$$

where $\hat{n}(s)$ and $\hat{d}(s)$ are polynomials in s, and where the continuous $\varphi(\sigma)$ is such that

$$0 \leq \sigma\varphi(\sigma) \leq \beta\sigma^2.$$

Assume that $\hat{g}_a(s) \in \hat{\mathcal{A}}$ and that $\hat{g}(s)$ has no poles with positive real parts. Under these conditions the system is $\mathcal{L}_2$-stable if

$$\inf_{\omega>0} Re[\hat{g}(j\omega)] + \frac{1}{\beta} > 0. \quad \square$$

Proof: See [18], Section 6.7. It is noted that a transfer function $\hat{g}_a(s) \in \hat{\mathcal{A}}$ whenever it is asymptotically stable and proper [18]. In addition, $u_1 \in \mathcal{L}_2$ and $u_2 \in \mathcal{L}_2$ are required to conclude that $y_1 \in \mathcal{L}_2$ and $y_2 \in \mathcal{L}_2$.

B. Signals and Block Diagram

A pre-requisite for the stability analysis is to redraw Fig. 1 to the structure of Fig. 2 and define the quantities of Fig. 2 in terms of those in Fig. 1. This is done using re-ordering of linear blocks according to the superposition principle, and using the fact that delays can be interchanged with static nonlinear blocks. This leads to the block diagram of Fig. 3. It follows immediately from Fig. 3 that

$$u_1(s) = e^{-sc_{k_p}T_S}\left(n_{k_p}P_{k_p,max}(s) - \Delta P_{blank}(s)\right)$$

$$+(I+N)(s) + \tilde{P}_p(s) + \sum_{k_p \neq k=1}^{K} n_k e^{-sc_k T_S} P_k(s), \quad (12)$$

$$u_2(s) = e^{-sc_{k_p}T_S} C(s) \Delta P_p^{ref}(s), \quad (13)$$

$$\hat{g}(s) = e^{-s(c_{k_p}+f_{k_p})T_S} C(s), \quad (14)$$

$$\varphi(u) = n_{k_p} q_{k_p}(u). \quad (15)$$

C. Assumptions

The following assumptions are then introduced to enable a verification of the conditions for the circle criterion:

- A4) $C(s) = \frac{K_P}{T_I}\frac{1}{s+\delta}$, $\delta > 0$.
- A5) $\varphi(u) = n_{k_p} q_{k_p,\varepsilon}(u)$, where $q_{k_p,\varepsilon}(u) \leq q_{k_p}(u)$ is continuous, $q_{k_p,\varepsilon}(u) \to q_{k_p}(u)$ when $\varepsilon \to 0$, and $q_{k_p,\varepsilon}(u)$ and $q_{k_p}(u)$ obey the same sector condition.
- A6) $P_{k_p,max}(s)$ is the Laplace transform of $H(t)P_{k_p,max}$, where $H(t)$ is the Heaviside function, and where the pole in 0 is replaced with $-\delta$, by replacement of s with $s+\delta$, $\delta > 0$.
- A7) $\Delta P_{blank}(s)$ is the Laplace transform of a signal generated by proper asymptotically stable filtering.
- A8) $(I+N)(s)$ is the Laplace transform of a signal generated by proper asymptotically stable filtering.
- A9) $\tilde{P}_p(s)$ is the Laplace transform of a signal generated by proper asymptotically stable filtering.
- A10) $P_k(s)$, $k_p \neq k = 1, ..., K$ are the Laplace transforms of signals generated by proper asymptotically stable filtering.
- A11) $\Delta P_p^{ref}(s)$ is the Laplace transform of $H(t)\Delta P_p^{ref}$, where the pole in 0 is replaced with $-\delta$, by replacement of s with $s+\delta$, $\delta > 0$.

The parameter $\delta > 0$ in A4, A6 and A11 ensures asymptotic stability, therefore the main result becomes a conjecture when $\delta \to 0$. A5 is needed to obtain the smoothness required by Lemma 1. A6 and A11 ensure strict properness. They hold since the control loop is started at time 0. A7-A10 are standard signal conditions that together with A6 and A11 ensure that (12) and (13) meet $u_1 \in \mathcal{L}_2$ and $u_2 \in \mathcal{L}_2$.

D. Main Result

Theorem 1: Assume that A1-A11 hold, β is given by (16), and $\delta > 0$ is small. Then the feedback control loop of Fig. 1 with $q_{k_p,\varepsilon}(\cdot)$ replacing $q_{k_p}(\cdot)$ is globally $\mathcal{L}_2$-stable provided that

$$\left(\beta\frac{K_P}{T_I}\right)\left((c_{k_p}+f_{k_p})T_S\right) < 1. \quad \square$$

Proof: The conditions underpinning Lemma 1 are first verified, using A1-A11. Starting with $\hat{g}(s)$ of (14), asymptotic stability and (strict) properness follow from A4. Since $\hat{g}(s)$ neither contains unstable poles nor impulses, $\hat{g}(s) \in \mathcal{A}$. A6-A10 and (12) show that $u_1(s)$ is a sum of Laplace transforms that are all formed by asymptotically stable and proper filtering, hence $u_1 \in \mathcal{L}_2$. The same is true for $u_2(s)$, referring to A4, A11 and (13). Fig. 4 illustrates the static nonlinearity $\varphi(u) = n_{k_p} q_{k_p}(u)$. Note that by (6) and (8), the nonlinearity is designed with zero output when $u(t)$ commands less than one RBG, as well as when $u(t) > 0$. This ensures that the red and blue sector bounds always exist, hence the sector condition is always fulfilled. The quantization and requirement on continuity is handled by A5, with the consequence that the stability result needs to be understood as a limiting case when $\varepsilon \to 0$. The slope of the blue sector bound follows from (7), (9), the value of n_{k_p}, and by noting that $Q_{k_p,PRB}$ PRBs remain to the left of the leftmost falling edge of the quantizer. The slope is

$$\beta = n_{k_p}\frac{q_{k_p,min}}{u_{k_p,min} + Q_{k_p,PRB}}$$

$$= n_{k_p}\frac{10\log_{10}\left|\frac{m_{k_p,min}+1}{m_{k_p,max}}\right|}{\left(m_{k_p,min}+1-m_{k_p,max}\right)Q_{k_p,PRB}}. \quad (16)$$

This proves that the circle criterion holds for Fig. 1.

The stability can then be analysed using Lemma 1. Referring to (14) and A4, the real part of the loop gain becomes

$$Re[g(\hat{j\omega})] = Re[\frac{K_P}{T_I}\frac{e^{-j\omega(c_{k_p}+f_{k_p})T_S}}{j\omega+\delta}]$$

$$\frac{-K_P}{T_I}\frac{\omega sin(\omega(c_{k_p}+f_{k_p})T_S)}{\omega^2+\delta^2}$$

$$+\frac{K_P}{T_I}\frac{\delta cos(\omega(c_{k_p}+f_{k_p})T_S)}{\omega^2+\delta^2}, \ \forall\omega. \quad (17)$$

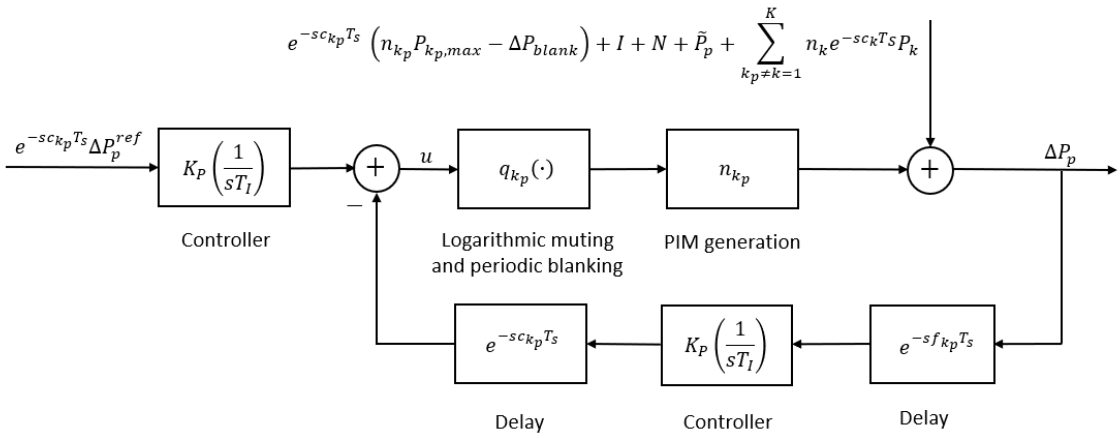

Fig. 3. The block diagram of the single carrier PIM power feedback control system, redrawn for $\mathcal{L}_2$ stability analysis.

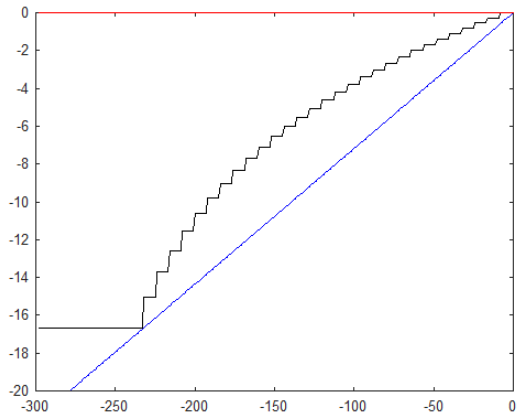

Fig. 4. The static nonlinearity $\varphi(u)=n_{k_p}q_{k_p}(u)$ for $n_{k_p}=2$ together with the sector bounds (red and blue). The parameters of (6)-(10) were $m_{k_p,min}=4$, $m_{k_p,max}=34, Q_{k_p,PRB}=8$.

After some rearrangements, (17) and the circle criterion leads to the stability condition

$$-sin(\omega(c_{k_p}+f_{k_p})T_S) > -\left(\frac{K_P}{T_I}\right)^{-1}\frac{1}{\beta}\omega$$
$$-\left(\frac{K_P}{T_I}\right)^{-1}\frac{\delta^2}{\beta}\frac{1}{\omega}-\delta cos(\omega(c_{k_p}+f_{k_p})T_S)\frac{1}{\omega},\quad \forall\omega>0. \tag{18}$$

Two cases arise, depending on the last term of (18).

First, in case $\omega \leq (\pi/(2(c_{k_p}+f_{k_p})T_S)$ it follows from the signs of the right hand side terms of (18) that if

$$-sin(\omega(c_{k_p}+f_{k_p})T_S) > -\left(\frac{K_P}{T_I}\right)^{-1}\frac{1}{\beta}\omega, \tag{19}$$

holds, then the stability condition of (18) also holds. Proceeding with (19), the functions of the right and left hand sides intersect at $\omega=0$. Therefore, if the slope of $-sin(\omega(c_{k_p}+f_{k_p})T_S)$ is less negative than $-\left(K_P/T_I\right)^{-1}\beta^{-1}\omega$, then there are no further intersections between the functions of (19) for $\omega>0$, since the slope of $-sin(\omega(c_{k_p}+f_{k_p})T_S)$ is minimal in $\omega=0$ and equal to $-(c_{k_p}+f_{k_p})T_S$. Bounding (19) with the minimum gives the condition

$$-(c_{k_p}+f_{k_p})T_S > -\left(\frac{K_P}{T_I}\right)^{-1}\frac{1}{\beta}. \tag{20}$$

Now (20) implies (19) and thereby (18). (20) can be rearranged into the following loop-gain-loop-delay stability condition for the first case

$$\left(\beta\frac{K_P}{T_I}\right)\left((c_{k_p}+f_{k_p})T_S\right) < 1. \tag{21}$$

Proceeding with the second case, it is first noted that according to case 1 (21) needs to hold for $\omega \leq (\pi/(2(c_{k_p}+f_{k_p})T_S)$. Since (21) is independent of ω, it is assumed for $\omega \geq (\pi/(2(c_{k_p}+f_{k_p})T_S)$ as well. The different terms of (18) can now be bounded for $\omega \geq (\pi/(2(c_{k_p}+f_{k_p})T_S)$.

The minimum value of the left hand side term $-sin(\omega(c_{k_p}+f_{k_p})T_S)=-1$, which is obtained for example for $\omega=(\pi/(2(c_{k_p}+f_{k_p})T_S)$. The first term of the right hand side of (18) can be estimated as

$$-\left(\frac{K_P}{T_I}\right)^{-1}\frac{1}{\beta}\omega < -\left(\frac{K_P}{T_I}\right)^{-1}\frac{1}{\beta}\frac{\pi}{2(c_{k_p}+f_{k_p})T_S} < -\frac{\pi}{2}. \tag{22}$$

where the last inequality follows by (21). Hence, by (22)

$$-sin(\omega(c_{k_p}+f_{k_p})T_S)$$
$$+\left(\frac{K_P}{T_I}\right)^{-1}\frac{1}{\beta}\omega > \frac{\pi}{2}-1,\ \omega \geq \frac{\pi}{2(c_{k_p}+f_{k_p})T_S}. \tag{23}$$

Since $\omega \geq (\pi/(2(c_{k_p}+f_{k_p})T_S)$, it follows that the absolute value of the two remaining terms of the right hand side of (18) can be made smaller than $\frac{\pi}{2}-1$ by selection of a small enough $\delta>0$. Therefore (21) implies that (18) holds for $\omega \geq (\pi/(2(c_{k_p}+f_{k_p})T_S)$ as well. This proves Theorem 1.

E. Implementation

The feedback loop is tuned as follows. The delays, sampling period and actuator parameters are constants determined by the wireless system implementation. The user can

select T_I accounting for measurement filtering needs. The gain K_P can then be computed from Theorem 1, if preferred with a margin. The continuous time control system also needs to be discretized. This is performed with the stability preserving Tustin's approximation [14].

V. Multiple radio carriers

A. Optimal Dual Carrier Muting

To understand how the logarithmic feedback control algorithm of Section III can be generalized to multiple DL carriers, the dual carrier case is analysed. The problem to maximize the relative throughput

$$V(\bar{q}_1(t), \bar{q}_2(t)) = \bar{q}_1(t) + \bar{q}_2(t), \tag{24}$$

is considered, noting that $\bar{q}_1(t) + \bar{q}_2(t)$ measures the allowed fraction of the DL bandwidth. A division of (2) without modeling errors, with (1), results in the main constraint which completes the throughput maximization problem:

$$\begin{pmatrix} \hat{\bar{q}}_1(t) \\ \hat{\bar{q}}_2(t) \end{pmatrix} = \arg \max_{\bar{q}_1(t), \bar{q}_2(t)} V(\bar{q}_1(t), \bar{q}_2(t)) \tag{25}$$

subject to

$$(\bar{q}_1(t))^{n_1} (\bar{q}_2(t))^{n_2} = \bar{\Delta} \tag{26}$$

$$\bar{q}_1(t) \in [\bar{q}_{1,min}, 1], \ \bar{q}_{1,min} \geq 0 \tag{27}$$

$$\bar{q}_2(t) \in [\bar{q}_{2,min}, 1], \ \bar{q}_{2,min} \geq 0. \tag{28}$$

Here $0 \leq \bar{\Delta} \leq 1$ expresses the desired PIM power reduction. Note that the main constraint represents a *full buffer traffic* case, i.e. a 100 % traffic case, since the muting of Section III is by means of a scheduler threshold. To proceed, the following assumption is introduced:

A12) The DL carriers of the PIM product term are sorted in descending order of the size of their exponents, and $k_p = 1$.

The following result states that the optimal solution is to apply a greedy algorithm in the PIM product degrees:

Theorem 2: Consider the problem (25)-(28), assume that A1 and A12 holds and that $n_1 \geq n_2$. Then it is optimal to first mute carrier 1 as much as needed or as much as allowed by $\bar{q}_{1,min}$. If more muting is needed, carrier 2 is muted as much as needed or as much as allowed by $\bar{q}_{2,min}$ $\square$.

Proof: To solve the optimization problem, $\bar{q}_2(t)$ is obtained from (26) and inserted into (24), resulting in the one dimensional loss function

$$V(\bar{q}_1(t)) = \bar{q}_1(t) + \bar{\Delta}^{\frac{1}{n_2}} (\bar{q}_1(t))^{-\frac{n_1}{n_2}}. \tag{29}$$

Any maximizing point in the interior region of (27) and (28) needs to fulfil

$$\frac{dV}{d\bar{q}_1(t)} = 1 + \bar{\Delta}^{\frac{1}{n_2}} \left(-\frac{n_1}{n_2} \right) (\bar{q}_1(t))^{-\left(\frac{n_1}{n_2}+1\right)} = 0. \tag{30}$$

However, another differentiation results in

$$\frac{d^2V}{d\left(\bar{q}_1(t)\right)^2} = \bar{\Delta}^{\frac{1}{n_2}} \left(\frac{n_1}{n_2} \right) \left(\frac{n_1}{n_2} + 1 \right) (\bar{q}_1(t))^{-\frac{n_1}{n_2}+2} > 0 \tag{31}$$

by (27) and (28) and since $\bar{\Delta} \geq 0$. Therefore, there cannot exist an interior maximum point and the maximum solution must occur on the boundary of (27) and (28). To find the optimum, all possibilities need to be evaluated and the best one found. The rectangular boundary defined by (27) and (28) give the cases of Table I. The value of the criterion function for a row is the sum of the first and second columns of that row. The cases of Table I may impose simple constraints on $\bar{\Delta}$, the second case e.g. requires that $\bar{\Delta} \leq \bar{q}_{1,min}^{n_1}$. The proof now makes extensive use of

TABLE I
Boundary Cases Defined By (26), (27) And (28)

$\hat{\bar{q}}_1(t)$	$\hat{\bar{q}}_2(t)$
1	$max\left(\bar{q}_{2,min}, \bar{\Delta}^{\frac{1}{n_2}}\right)$
$\bar{q}_{1,min}$	$max\left(\bar{q}_{2,min}, \bar{\Delta}^{\frac{1}{n_2}} \bar{q}_{1,min}^{-\frac{n_1}{n_2}}\right)$
$max\left(\bar{q}_{1,min}, \bar{\Delta}^{\frac{1}{n_1}}\right)$	1
$max\left(\bar{q}_{1,min}, \bar{\Delta}^{\frac{1}{n_1}} \bar{q}_{2,min}^{-\frac{n_2}{n_1}}\right)$	$\bar{q}_{2,min}$
1	1
1	$\bar{q}_{2,min}$
$\bar{q}_{1,min}$	1
$\bar{q}_{1,min}$	$\bar{q}_{2,min}$

the facts that for $n > 0, n_1 > 0, n_2 > 0$ it holds that $0 < x^{\frac{1}{n}} \leq 1, x \in (0,1]$; $x^{\frac{1}{n}}, x \in (0,1]$ is increasing; and $n_1 > n_2 \Rightarrow x^{\frac{1}{n_1}} > x^{\frac{1}{n_2}}, x \in (0,1)$.

The solution to (25)-(28) is investigated by decreasing $\bar{\Delta}$ from 1. For $\bar{\Delta} = 1$, only case 5 of Table I applies, and $V(\hat{\bar{q}}_1(t), \hat{\bar{q}}_2(t)) = 2$. When $\bar{\Delta}$ is decreased so that neither $\bar{q}_{1,min}$ nor $\bar{q}_{2,min}$ is reached, cases 1 and 3 apply. It follows by (24), A12 and the properties listed above that

$$V(\bar{\Delta}^{\frac{1}{n_1}}) \geq V(\bar{\Delta}^{\frac{1}{n_2}}), \tag{32}$$

and therefore the choice is to mute the carrier with the largest exponent, i.e. case 3, until $\bar{q}_{1,min}$ is reached, i.e. case 7 is reached. When $\bar{\Delta}$ is further decreased case 2 applies until $\hat{\bar{q}}_2(t) = \bar{q}_{2,min}$ and case 8 is reached, and no more muting is possible. This is the algorithm stated by Theorem 2.

B. Random Traffic Compensation

Theorem 2 builds on a full buffer assumption. Whenever more than one carrier needs to be muted, the feedback loop of the main carrier is broken which means that the threshold acts on varying traffic that may be modeled as random. The same is true for the thresholds of the remaining carriers. A compensation for the full buffer traffic is therefore needed to control the traffic that is to be rejected more accurately.

For following random traffic is therefore assumed

A13) $\bar{P}_k(t) = \bar{p}_k(t) \bar{P}_{k,max}, \ \ \bar{p}_k(t) \in U(0,1)$.

Here $U(0,1)$ is the uniform distribution, which is a flat prior for the DL powers. Assuming that Theorem 2 would produce a threshold $\hat{\bar{q}}_k(t)$, acting on the traffic of carrier k, the expected normalized remaining power becomes

$$E\left[\bar{p}_k(t) | \hat{\bar{q}}_k(t)\right]$$

$$= \int_0^1 p p_U(p|\hat{\bar{q}}_k(t))dp = \int_0^{\hat{\bar{q}}_k(t)} p1dp = \frac{\hat{\bar{q}}_k^2(t)}{2}. \quad (33)$$

One alternative to compensate for varying traffic would be to use the loss of muted power, as compared to the full buffer case compensation. However, that would lead to compensation even without muting in the full buffer case since the maximum value of (33) is 0.5. This is not desirable. A more soft compensation is therefore selected from (33), using $\hat{\bar{q}}_k(t) = 1$ to represent the maximum power case. The relative loss of remaining power then becomes

$$\ell(t) = \frac{1}{2} - \frac{\hat{\bar{q}}_k^2(t)}{2} = \frac{1 - \hat{\bar{q}}_k^2(t)}{2}. \quad (34)$$

C. The Degree Greedy Algorithm

To define the degree greedy PIM-A algorithm in the general case with K carriers, it is conjectured that Theorem 2 generalizes to K carriers. The total amount of muting computed by the feedback controller of Section III is denoted $\bar{q}_{tot}(t)$, while the total amount allocated in the algorithm so far is denoted $\bar{q}_{acc}(t)$. Two additional effects need to be accounted for. First, the total muting command of the feedback loop relates to $n_1 = n_{k_p}$, by A12. Since, by (2)

$$\frac{\partial P_p(t)}{\partial q_k(t)} / \frac{\partial P_p(t)}{\partial q_1(t)} = \frac{n_k}{n_1}\frac{q_1(t)}{q_k(t)} \approx \frac{n_k}{n_1}, \quad (35)$$

it follows that the muting for carrier k needs to be scaled up with an approximate factor of n_1/n_k. The last approximation of (35) is motivated by simplicity, noting that there are already several simplification involved. The accumulated muting needs inverse scaling. Secondly, the muting for carrier k needs to be compensated for by (34). This leads to a compensated muting command equation

$$\hat{\bar{q}}_k(t) = 1 - \frac{n_1}{n_k}\left(\frac{\bar{q}_{tot}(t) - \bar{q}_{acc}(t)}{\ell(t)}\right). \quad (36)$$

Inserting (34) leads to the third degree equation

$$\frac{1}{2}\left(1 - \hat{\bar{q}}_k(t)\right)^2\left(1 + \hat{\bar{q}}_k(t)\right) = \frac{n_1}{n_k}\left(\bar{q}_{tot}(t) - \bar{q}_{acc}(t)\right). \quad (37)$$

This equation could be solved analytically with techniques of Thomas Harriot, [7], cf. Wikipedia. To obtain an elementary solution, the approximation $(1 + \hat{\bar{q}}_k(t)) \approx 1$ is used, which gives

$$\hat{\bar{q}}_k(t) = 1 - \sqrt{\frac{2n_1}{n_k}\left(\bar{q}_{tot}(t) - \bar{q}_{acc}(t)\right)}. \quad (38)$$

Assuming that A12 and A13 hold, the algorithm of Theorem 2 can now be generalized to the algorithm of Table II.

D. Implementation

The feedback control of the main carrier results in a control signal $u(t)$ which is input to the degree greedy algorithm. The outputs of the algorithm are new distributed muting commands, $\hat{\bar{q}}_k(t)$, that are sent to each carrier.

TABLE II
DEGREE GREEDY ALGORITHM

Initialization

$\bar{q}_{tot}(t) = \frac{|u(t)|}{m_{1,max}Q_{1,PRB}}$
$\bar{q}_{acc}(t) = 0.0$
$\hat{\bar{q}}_k(t) = 1.0,\ k = 1, ..., K$
$ready = false$
$k = 1$

Main Carrier

$if\ \bar{q}_{1,min} < 1 - \frac{n_1}{n_1}\left(\bar{q}_{tot}(t) - \bar{q}_{acc}(t)\right)$
  $\hat{\bar{q}}_1(t) = 1 - \frac{n_1}{n_1}\left(\bar{q}_{tot}(t) - \bar{q}_{acc}(t)\right)$
  $ready = true$
$else$
  $\hat{\bar{q}}_1(t) = \bar{q}_{1,min}$
  $\bar{q}_{acc}(t) = \bar{q}_{acc}(t) + \frac{n_1}{n_1}\left(\frac{1}{2} - \frac{1}{2}\hat{\bar{q}}_1^2(t)\right.$
end

Secondary Carriers

$while\ (k \le K)\ and\ (not\ ready)$
  $if\ k > 1$
    $if\ \bar{q}_{k,min} < 1 - \sqrt{\frac{2n_1}{n_k}\left(\bar{q}_{tot}(t) - \bar{q}_{acc}(t)\right)}$
      $\hat{\bar{q}}_k(t) = 1 - \sqrt{\frac{2n_1}{n_k}\left(\bar{q}_{tot}(t) - \bar{q}_{acc}(t)\right)}$
      $ready = true$
    $else$
      $\hat{\bar{q}}_k(t) = \bar{q}_{k,min}$
      $\bar{q}_{acc}(t) = \bar{q}_{acc}(t) + \frac{n_k}{n_1}\left(\frac{1}{2} - \frac{1}{2}\hat{\bar{q}}_k^2(t)\right.$
      $k = k + 1$
    end
  $else$
    $k = k + 1$
  end
end

VI. Performance

A. Simulation Assumptions

The interference $\bar{I}(t)$ was generated with simulation of four neighbour cell UEs with Doppler fading frequencies of $2, 3, 7$ and 15 Hz, with bursty interference powers of 0.1 W. The path-losses were $25, 30, 35$ and 40 dBs below the served UE used for measurement of average signal to noise and interference ($SINR$) power. The UL receiver had a noise figure of 3 dB. All carriers used bandwidths of 100 MHz and had maximum powers of $P_{k,max} = 20$ dBW. The PIM signal was generated using a fading channel with a Doppler frequency of 1 Hz. The actuator used $m_{k_p,min} \in [4, 33]$, $m_{k_p,max} = 34$, $Q_{k_p,PRB} = 8$, and $n_{k_p} = 3$ from which β of (16) was computed for *varying* $m_{k_p,min}$ and corresponding $q_{1,min}$. The controller used $T_S = 0.050$ s, $c_{k_p} = 0.04$, $f_{k_p} = 0.96$, and $T_I = 0.50$ s. K_p was then computed from the loop-gain-loop-delay stability condition of Theorem 1, which therefore also provides a unique tuning of the feedback loop.

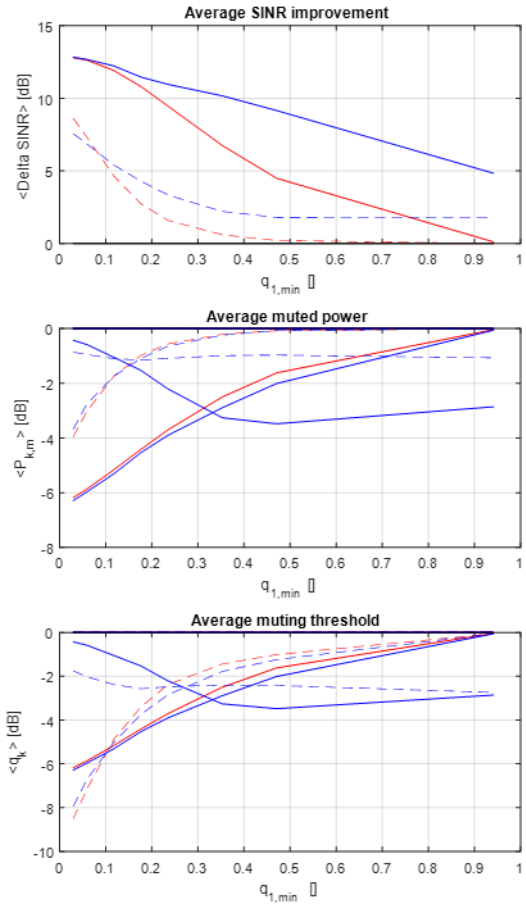

Fig. 5. Performance of IM5 PIM-A, as a function of the allowed muting of the main feedback control carrier. Single carrier (red), multiple carrier (blue), full buffer traffic (solid) and varying traffic (dashed). The multiple blue curves in the middle and bottom plots represent the two DL carriers.

B. Effect of Muting Limitations

The performance evaluation addresses the effect of $q_{1,min}$. IM5 PIM with $n_1 = 3$, $n_2 = 2$ was studied. The average loss of SINR due to PIM was scaled to 15 dB for full buffer traffic and 9 dB for varying traffic. The secondary carrier used a fix $m_{2,min} = 4$, while $m_{1,min}$ *was varied*. The results appear in Fig. 5. The gains are comparable to the PIM cancellation gains of [8]. However, the computational complexity of the PIM-A algorithm is many orders of magnitude smaller. The average SINR-improvement $< \Delta SINR >$ in the top figure is significantly larger for the degree greedy algorithm than for the single DL carrier feedback controller when run for the carrier with $n_1 = 3$. The difference levels out when $\bar{q}_{1,min} > 0.5$ and the secondary DL carrier is fully utilized.

There is a large performance difference between full buffer and varying traffic, between 6 and 8 dB for low $\bar{q}_{1,min}$. The explanation follows by a comparison of the bottom and middle plots - the average muted power for varying traffic is much below the corresponding thresholds $\hat{\bar{q}}_k(t)$.

VII. Conclusions

The proposed SISO and MISO PIM-A algorithms reduce PIM by feedback controlled data bandwidth muting of a single or multiple DL carriers. The logarithmic single carrier feedback control loop was proved to be $\mathcal{L}_2$-stable provided that a loop-gain-loop-delay condition holds. The optimal MISO algorithm was proved to be greedy in the exponents of the PIM product, enabling a SISO feedback controller reuse for MISO control. The performance evaluation indicated that the simulated traffic has a very significant impact, and motivates the use of the MISO controller for practical traffic.

Acknowledgment

The author thanks his manager M. Wargelius and product manager K. Kathuria for encouragement to publish, and Prof. B. Göransson for constructive comments.

References

[1] The 3GPP, "Universal Terrestrial Radio Access (E-UTRA); LTE physical layer; General description, 3GPP TS 36.201, release 12 (v. 12.2.0)," Mar. 2015. [Online]. Available: http://www.3gpp.org/DynaReport/36201.htm

[2] K. J. Åström and T. Hägglund, *Advanced PID Control.* Reasearch Triangle Park, NC: The Instrumentation, Systems and Automation Society, 2006.

[3] L. Dussopt and G. M. Rebeiz, "Intermodulation distortion and power handling in RF MEMS switches, varactors and tunable filters", *IEEE Trans. Microwave Theory and Techniques*, vol. 51, no. 4, pp. 1247-1256, 2003.

[4] A. Goldsmith, *Wireless Communications.* Cambridge, MA: Cambridge Univ. Press, 2005.

[5] G. C. Goodwin, M. M. Seron and J. A. DeDona, *Constrained Control and Estimation – An Optimization Approach*. London: UK, Springer, 2005.

[6] W. J. Hall, M. H. Gibson, M.A. Kunes, J. M. Eskell and G. G. Connor, "The control of passive intermodulation products in spacecraft antennas", In *Proc. IEE Colloquium on Passive Intermodulation Products in Antennas and Related Structures*, 1989.

[7] T. Harriot, *Artes Analyticae Praxis*, 1631.

[8] B. Jang, H. Kim, Y. Seo, S. Im and S. Hong, "Mitigation of the third-order passive intermodulation distortion interference on uplink signal", In *Proc. IEEE International Conference on Electronics, Information and Communication*, Auckland, New Zeeland, 2019.

[9] B. Jang, S. Im, C. Kim and S. Hong, "Modeling of passive intermodulation distortion using the neural networks and the cubic Volterra filter", In *Proc. IEEE International Conference on Information and Communication Technology Convergence*, Jeju, Korea, 2019.

[10] A. H. Jazwinski, *Stochastic Processes and Filtering Theory*. New York, NY, USA: Academic Press, 1970.

[11] T. Kimono and N. Kuga, "Basic consideration on non-contact localization for a PIM source in antenna array", In *Proc. IEEE International Symposium on Antennas and Propagation*, Osaka, Japan, 2020.

[12] C. Kudsia, R. Cameron and W. -C. Tang, "Innovations in microwave filters and multiplexing networks for communications satellite systems", *IEEE Trans. Microwave Theory and Techniques*, vol. 40, no. 6, pp. 1133-1149, 1992.

[13] Y. Leost, M. Abdi, R. Richter and M. Jeschke, "Interference rejection combining in LTE networks", *Bell Labs Techn. J.*, vol. 17, no. 1, pp. 25-49, 2012.

[14] A. V. Oppenheim and R. W. Schafer, *Digital Signal Processing*. Englewood Cliffs, NJ: Prentice Hall, 1975.

[15] W. Rudin, *Principles of Mathematical Analysis*. New York, NY: Mc Graw Hill, 1976.

[16] M. H. Stone, "The generalized Weierstrass approximation theorem", *Mathematics Mag.*, vol. 21, no. 4, pp. 167-184, 1948.

[17] R. S. Sutton and A. G. Barto, *Reinforcement Learning – An Introduction*. Cambridge, MA: MIT Press, 2020.

[18] M. Vidyasagar, *Nonlinear Systems Analysis*. Englewood Cliffs, NJ: Prentice Hall, 1978.